Use of Infrared Bands of the Surfactant Headgroup to Identify Mixed Surfactant Structures Adsorbed on Titania

Haiyan Li and Carl P. Tripp*

Laboratory for Surface Science and Technology and Department of Chemistry, University of Maine, Orono, Maine 04469

Received: July 22, 2004

Attenuated total reflection-Fourier transform infrared spectroscopy (ATR-FTIR) was used to identify the mixed surfactant structures formed on charged TiO_2 particles. Cetyltrimethylammonium bromide (CTAB) was first added to a bare TiO_2 surface at three different solution concentrations that result in adsorbed hemimicelle, admicelle, or micelle structures. Each CTAB structure was then probed as a function of contact time with a solution containing the deuterated form of the anionic surfactant, sodium dodecyl sulfate (SDS). While the amount of CTAB and SDS was determined from the intensity of the strong CH_2 and CD_2 stretching modes, it is the headgroup bands that provide the important structural information on the mixed surfactant architectures. By measuring the changes in the headgroup bands for both SDS and CTAB along with the change in the adsorbed amount of each surfactant as a function of time, a clearer picture emerges of the mixed surfactant structures formed on the surface.

Introduction

Mixtures of polymers and surfactants are used extensively to modify the colloidal behavior of particulate suspensions.[1−5] However, the relationship between the complex surfactant/polymer interactions on surfaces and their interfacial properties is an area that is not well understood. This area of research would clearly benefit from the development of new methods and techniques that can be used to identify the molecular structures and dynamics of surfactant/polyelectrolyte mixtures on surfaces. In this regard, we recently have established an infrared (IR) spectroscopic approach that can be used to detect surfactants and polymers adsorbed on TiO_2 particulates from aqueous solutions.[6] The technique is based on the use of attenuated total reflection (ATR) in which a ZnSe crystal is coated with high surface area TiO_2 particles. The approach is not limited to TiO_2, as polymer/surfactant adsorption was extended to a SiO_2 interface by converting the TiO_2 surface to SiO_2 using atomic layer deposition.[7] Alternatively, adsorption onto other high surface area particles can be studied spectroscopically by using a polymer binder to anchor the particles onto the ZnSe crystal.[8] An attraction of the IR-ATR approach is that the amount of each adsorbate can be monitored separately when the particles are exposed to mixtures of surfactants and polymers. There is an additional advantage when the ATR technique is applied to the adsorption onto particles bound to the ATR crystal. In this case, the higher surface area associated with the particles enables detection of the weak, yet information-rich headgroup IR bands of surfactants. The high surface area also provides good signal-to-noise in detection of the strong CH_2 stretching modes during time-dependent measurements of the adsorbed amount.[9]

In one ATR study, CTAB was added to negatively charged TiO_2 particles at a solution concentration where hemimicelles form on the surface.[6] The CTAB structure on the surface was then probed by adding a solution containing SDS. It was shown that the nature of the aggregated CTAB structure and not the adsorbed amount dictated the quantity of SDS incorporated into the CTAB layer. In this study, structural data were inferred from the frequency shift in the CH_2 stretching modes. The CH_2 stretching bands near 2922 and 2850 cm^{-1} are generally the strongest bands in the spectra. The frequencies and widths of these bands are sensitive to the gauche/trans conformer ratio of the methylene chains, exhibiting a shift to lower frequencies characteristic of highly packed, all trans conformations.[6,10−12] However, the shifts in position of the CH_2 stretching modes are not very sensitive to different structures in pure surfactant systems. For example, the frequency position for solutions containing free CTAB or CTAB micelles appear at the same frequency.[11,12] This is because the packing density in the CTAB micelle is not sufficient to produce a frequency change in the CH_2 stretching modes. It was only in more highly packed mixed cationic/anionic surfactant structures that a shift in frequency was detected.[6,11]

A typical approach to obtaining structural information in ATR−IR measurements is to record spectra using polarized light. For example, the intensity ratio of the CH_2 stretching mode for a surfactant on a surface of an oxidized silicon ATR crystal recorded using parallel or perpendicular polarized light provided a means for determining the average orientation of a surfactant molecule on a surface.[13−15] However, these polarization measurements require a flat surface and therefore are not applicable for surfactants adsorbed on TiO_2 powders deposited on an ATR surface. Given the insensitivity of the position of the CH_2 bands to pure surfactant structures and the ineffectiveness of polarization studies, it appeared that an ATR method using powders would not provide information on the nature of aggregated surfactant structures. However, more recent work showed that the weak headgroup bands located in the 1450−1300 cm^{-1} range provided the key information on the nature of the aggregated CTAB structure.[9] The CTAB headgroup bands of particular importance are the δ_{as} $^+N-CH_3$ located at 1490 and

* Corresponding author. Phone: (207) 581-2235. Fax: (207) 581-2255. E-mail: ctripp@maine.edu.

10.1021/jp046741u CCC: $27.50
Published on Web 11/03/2004

1479 cm^{-1} and the δ_s $^+N-CH_3$ located at 1396 cm^{-1}, and the transition dipole moment vectors associated with the δ_{as} and δ_s are orthogonal to each other as shown in Scheme 1.

SCHEME 1: Transition Dipole Moment Vectors for $^+$N-CH_3 Bending Modes of CTAB

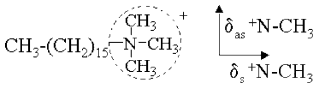

Much of our understanding on the relationship between the CTAB headgroup band intensity/frequency and surfactant structure is derived from the seminal and detailed IR studies of solutions containing CTAB micelles and mixed CTAB/SDS micelles by Sheuring and Weers[11] and Mantsch et al.[12] These solution-based studies provided the framework for structural interpretation for CTAB adsorbed on TiO_2. For example, Sheuring and Weers showed that the intensity of the δ_s $^+N-CH_3$ at 1396 cm^{-1} of CTAB micelles in solution increased with the addition of simple salts such as NaCl. Since the transition dipole associated with the δ_s $^+N-CH_3$ points outward from the micelle surface, they concluded that the intensity of this band would increase with the positioning of an oppositely charged ion in the same direction as the transition moment vector.

By analogy, the adsorption of CTAB directly interacting with the negative sites on a surface would also lead to an increase in the δ_s $^+N-CH_3$ mode located at 1396 cm^{-1}. This change in intensity of the δ_s $^+N-CH_3$ mode has been shown to occur with CTAB adsorption on negatively charged TiO_2 particles.[9] Specifically, abrupt changes in the 1396/2850 intensity ratio were shown to coincide with the abrupt changes in the adsorption isotherm, which in turn, have been attributed to different aggregated CTAB structures on the surface. The calculated ratio of the 1396/2850 band was used instead of the intensity of the 1396 cm^{-1} band because the ratio provided a relative measure of the percentage of the total absorb CTAB molecules directly interacting with charged surface sites. We recall that the intensity of the CH_2 mode at 2850 cm^{-1} is proportional to the number of CTAB molecules on the surface. At low CTAB concentration, a high 1396/2850 ratio was obtained, and this translated to a high percentage of the total adsorbed CTAB bound through direct interaction with the charged surface sites. In contrast, at high CTAB concentration, CTAB micelles adsorb on the TiO_2. In this case, a small percentage of the total number of CTAB molecules is involved in direct interaction with surface sites. This results in a low 1396/2850 intensity ratio.

This rich information content on the nature of the self-assembled architecture gleaned from analysis of the CTAB headgroup region has led to this study of the interaction of the CTAB layer with SDS. Our earlier work of SDS uptake into the adsorbed CTAB layer used the intensity of CH_2 stretching modes to measure adsorbed amount and the shift in the CH_2 stretching modes to determine packing density.[6] Structural information deduced from changes in the CTAB headgroups bands was not reported. We now reinvestigate the interaction of deuterated SDS adsorbed on TiO_2 with adsorbed CTAB hemimicelles with a focus on the structure interpretation of changes occurring in the headgroup region. Furthermore, we have extended this work to deuterated SDS uptake by CTAB admicelles and micelles adsorbed on TiO_2.

An important aspect of the work entails a detailed analysis of changes that occur in the SDS headgroup bands when mixed SDS/CTAB structures form on the surface. As with the CTAB headgroup bands, it is shown that changes in the SDS headgroup bands provide information on the nature of the aggregated structure. By examining the changes occurring to infrared bands due to the CTAB and SDS headgroups, along with the adsorbed amounts determined from the intensity of the CH_2 and CD_2 stretching bands, a clearer picture emerges on the type of mixed architectures that occur on a charged metal oxide surface.

Experimental Procedures

Fumed titania powder (P_{25}) was obtained from Degussa and used as received. The P25 powder has a BET N_2 surface area of 50 m^2/g and a measured isoelectric point (IEP) of 6.5. Cetyltrimethylammonium bromide (CTAB) and sodium dodecyl sulfate (SDS) were obtained from Aldrich. CTAB was recrystallized twice with an acetone/ethanol mixture, and SDS was double recrystallized with acetone.[6,9] Deuterated sodium dodecyl sulfate (d_{25}-SDS, 98.5% deuterated) was obtained from CDN Isotopes and used as received. The integrated intensity of the CH_2 stretching mode at 2850 cm^{-1} is used to compute the adsorbed amount of surfactant. Since this band is common to both SDS and CTAB, experiments were conducted using d_{25}-SDS in order to separately determine the adsorbed amount of SDS from the amount of adsorbed CTAB. The calibration procedure for converting the integrated intensity of the CD_2 and CH_2 stretching modes to an adsorbed amount of CTAB or SDS is described elsewhere.[6,9]

In brief, an ATR spectrum containing bands due to d_{25}-SDS and CTAB adsorbed on TiO_2 was recorded in the presence of pure water (i.e., no surfactant in the water). The ATR crystal was immediately removed from the cell and dried, and an absorbance spectrum was recorded through the ATR crystal containing the TiO_2 coating, CTAB, and d_{25}-SDS. The amount of CTAB and d_{25}-SDS was calculated by comparing the integrated intensity of the CH_2 or CD_2 band at 2850 and 2090 cm^{-1} to a Beer Law's plot obtained from absorbance spectra of known quantities of CTAB and d_{25}-SDS in KBr pellets. A baseline valley-to-valley integration from 2880 to 2830 cm^{-1} was used for the band at 2850 cm^{-1}. The corresponding integration limits for the 2090 cm^{-1} peak was 2130 and 2050 cm^{-1}. The amount of TiO_2 was computed in a manner similar to CTAB and d_{25}-SDS using the height of the Ti−O bulk mode at 635 cm^{-1}. Once the amount of CTAB and d_{25}-SDS on the dried ATR crystal was determined, these values were then used to calibrate the corresponding integrated intensities obtained in the original ATR spectrum recorded in water.

All solutions were made with deionized water (18 MΩ) obtained from a Milli-Q purification system. Solutions of NaOH and HCl were used to adjust the pH of the water and surfactant solutions. Unless stated, all experiments were carried out at pH 10.3, and at this pH, the titania surface is negatively charged.

ATR experiments were conducted using a standard ATR flow-through accessory obtained from Harrick mounted into a Bomem 110-E FTIR spectrometer. A ZeSe internal reflection element from Harrick was used and has a dimension of 50 × 10 × 2 mm with a 45° bevel. In coating the ZnSe crystal, a suspension was first prepared by adding 30 mg of the titania powder in 25 mL of methanol solution. The suspension was then placed in an ultrasonic bath for 30 min. A total of 200 uL of this solution was then deposited evenly on one side of ZnSe crystal. After the methanol evaporated, a robust thin film of titania (500 nm thickness) formed on the crystal surface.[6,9]

In a typical experiment, water adjusted to pH 10.3 was flowed at a rate of 5.8 mL/min through the ATR setup for at least 30 min. A reference spectrum was then recorded with the water flowing through the ATR cell. Next, a fresh CTAB solution at

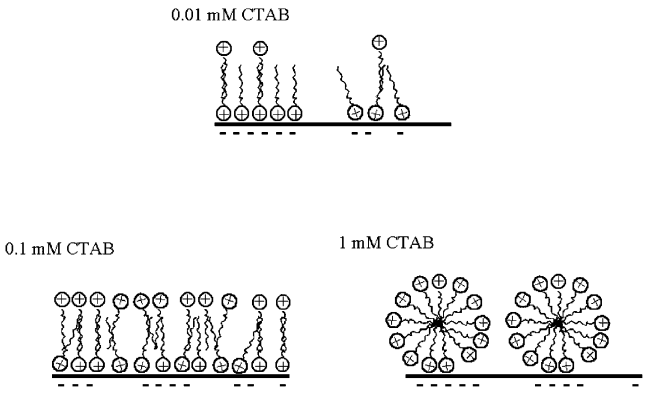

Figure 1. Hemimicellar, admicellar, and micellar structures formed on the TiO_2 surface at the indicated CTAB solution concentration.

a specified concentration was adjusted to pH 10.3 and then flowed into the ATR cell. Spectra were then recorded as a function of time for 2 h. The cell was then flushed with water for 1 min followed by addition of a fresh solution of d_{25}-SDS at the specified concentration and pH 10.3.

Experiments were conducted at three different CTAB and d_{25}-SDS solution concentrations. At the lowest concentrations (0.01 mM CTAB and 0.05 mM d_{25}-SDS), the spectral contributions from either d_{25}-SDS or CTAB in solution were not detected. However, at the higher solution concentrations (0.1 mM, 1 mM CTAB, and 0.5 mM, 5 mM d_{25}-SDS), the bands due to CTAB and d_{25}-SDS in solution did contribute to the overall spectrum. This spectral contribution from the CTAB or d_{25}-SDS in solution was determined by recording spectra through the ATR setup containing a bare TiO_2 coated ZnSe crystal at a pH where CTAB or d_{25}-SDS does not adsorb on TiO_2. For CTAB, this was pH = 3, and for d_{25}-SDS, the solution pH was 10.3. These spectra recorded for CTAB and d_{25}-SDS at different solution concentrations were then used to subtract out the spectral contribution from the surfactant in solution from the overall spectrum recorded during an adsorption experiment. It is noted that this correction was small, accounting for less than 10% of the total band intensity at the highest d_{25}-SDS and CTAB concentrations.

Results and Discussion

The amount of CTAB adsorbed on TiO_2 at pH 10.3 plotted as a function of log[CTAB] follows a double "S" curve having two sharp increases in adsorbed amount separated by plateau regions.[9] These two abrupt rises in the adsorbed amount are associated with the onset of formation of different aggregated structures. The three CTAB solution concentrations used in this study (0.01, 0.1, and 1.0 mM) were chosen because they lie in three different regions of the adsorption isotherm and thus result in the formation of different aggregated structures on the surface. The three structures formed on the surface in the order of increasing CTAB solution concentration have been attributed to hemimicelle, admicelle, and micelle structures (see Figure 1) on the surface, respectively.[9,16,17] A hemimicelle is described as a patchy bilayer in which the second layer is incomplete. The admicelle can be described as a more complete or less defective bilayer structure. At the highest CTAB concentration (1 mM), micelles adsorb on the surface.

The time-dependent change in the amount of CTAB adsorbed on TiO_2 at the three solution concentrations and the subsequent change in adsorbed amount of CTAB with the uptake of d_{25}-SDS are shown in Figures 2−4. In all three cases, the addition of d_{25}-SDS leads to an abrupt decrease in the amount of CTAB adsorbed on the TiO_2. It is noted that this decrease in the amount of CTAB on the surface is due to the uptake of d_{25}-SDS by the CTAB layer. This abrupt change in CTAB does not occur when pure water is flowed through the cell. Flowing water through the cell instead of the d_{25}-SDS solution leads to a slow and gradual decrease in the amount of CTAB adsorbed on TiO_2. It is also noted that the uptake of d_{25}-SDS is due to interaction with the CTAB structure on the surface and not due to adsorption of the d_{25}-SDS directly on the TiO_2. In a separate experiment, there was no adsorption of d_{25}-SDS when it was exposed to a bare TiO_2 surface at a solution pH of 10.3.

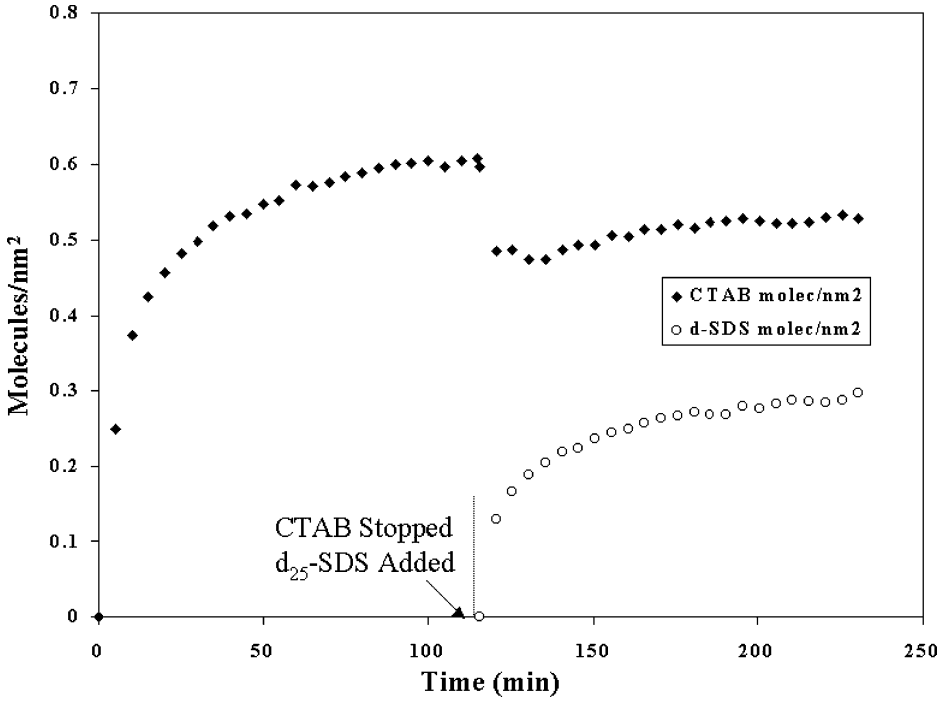

Figure 2. Time-dependent change in the amount of CTAB and d_{25}-SDS adsorbed on TiO_2 at pH 10.3 using a 0.01 mM CTAB solution followed by addition of 0.05 mM d_{25}-SDS solution.

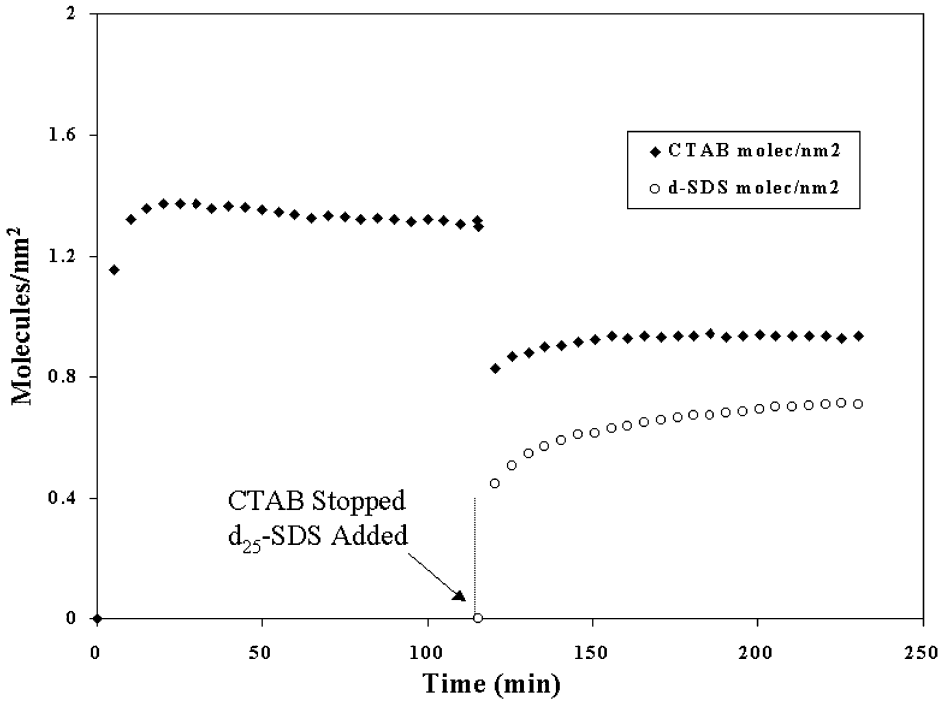

Figure 3. Time-dependent change in the amount of CTAB and d_{25}-SDS adsorbed on TiO_2 at pH 10.3 using a 0.1 mM CTAB solution followed by addition of 0.5 mM d_{25}-SDS solution.

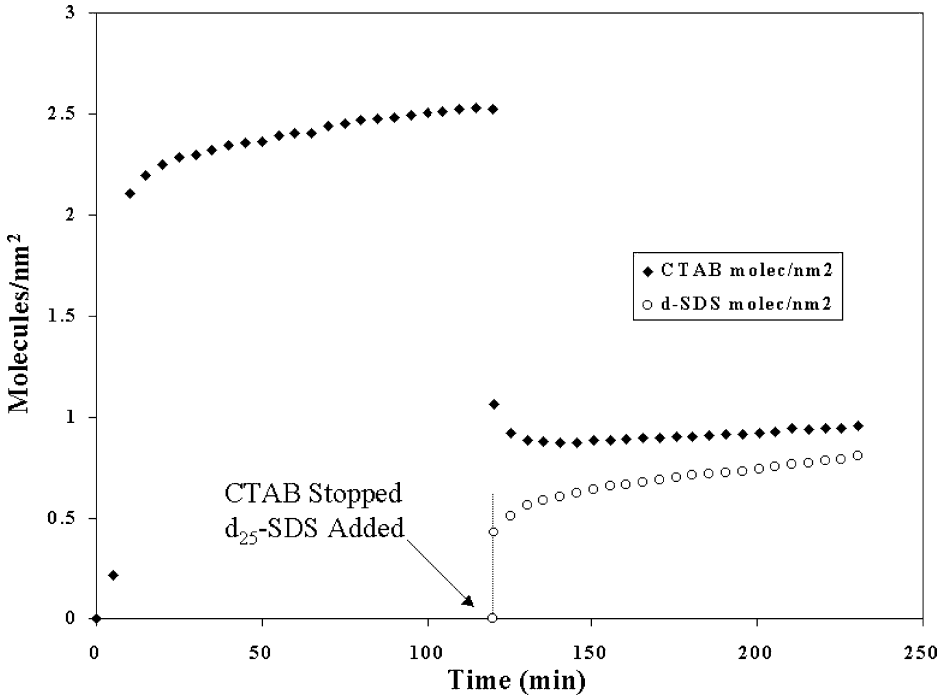

Figure 4. Time-dependent change in the amount of CTAB and d_{25}-SDS adsorbed on TiO_2 at pH 10.3 using a 1.0 mM CTAB solution followed by addition of 5.0 mM d_{25}-SDS solution.

Interaction of d_{25}-SDS with CTAB Hemimicelles Adsorbed on TiO_2. The changes in adsorbed amount of the two surfactants with the addition of 0.05 mM d_{25}-SDS solution to the hemimicelle CTAB adsorbed on TiO_2 is shown in Figure 2. Addition of the d_{25}-SDS solution to the preadsorbed CTAB layer results in the total uptake of about 0.29 molecules/nm^2 d_{25}-SDS and the removal of about 12% of the original amount of adsorbed CTAB. The final CTAB concentration is 0.53 CTAB molecules/nm^2; thus, a mixed surfactant structure is formed that is enriched in CTAB. The final CTAB/SDS number ratio is 1.8. Furthermore, the uptake of SDS is accompanied by a decrease in frequency in the CH_2 mode from 2922 to 2918 cm^{-1}. Actually, the addition of nondeuterated SDS leads to a shift of about 4 to 2918 cm^{-1}, while the addition of d_{25}-SDS leads to a shift of 2 to 2920 cm^{-1}, and the corresponding CD_2 mode shifts from 2195 to 2194 cm^{-1}. Experiments using nondeuterated SDS were performed to measure the total shift in CH_2 stretching modes for comparison of the overall packing densities of the three different SDS/CTAB mixed surfactant structures.

Incorporation of SDS has been attributed to favorable headgroup−headgroup and tail−tail interactions with the patchy second layer of the hemimicellar structure. The qualitative

picture proposed by Ninness et al.[6] is that a rapid adsorption of SDS produces highly ordered structures with the bilayer portion of CTAB hemimicelle (Scheme 2). The uptake of d_{25}-SDS in

SCHEME 2: Uptake of SDS by CTAB Hemimicelles

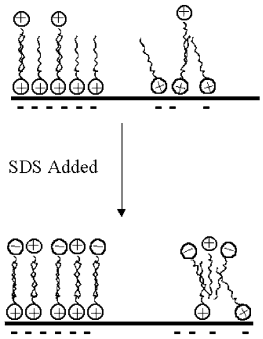

the second patchy CTAB layer would explain the low number of CTAB molecules expelled from the surface. In essence, the second patchy layer contains sufficient gaps to accommodate d_{25}-SDS. The favorable headgroup−headgroup and tail−tail interactions that occur with incorporation of the d_{25}-SDS into the second patchy layer would produce a more tightly packed mixed surfactant structure, as evidenced by the 4 cm^{-1} shift to lower frequency in the CH_2 antisymmetric stretching mode. Because the uptake of the d_{25}-SDS occurs primarily in the second layer, the overall mixed surfactant structure would be enriched in CTAB. This is consistent with the measured 1.8 CTAB/SDS number ratio. It is noted that Scheme 2 also shows some CTAB migration from the first layer to the second layer. This was not deduced from either the adsorbed amount data or frequency shift of the CH_2 modes but from changes in the headgroup bands. The information derived from the headgroup region will be discussed in a later section.

Interaction of d_{25}-SDS Solution with CTAB Admicelles Adsorbed on TiO_2. The change in the amount of CTAB adsorbed on TiO_2 in contact with a 0.1 mM CTAB solution at pH 10.3 is plotted in Figure 3. The plateau in the CTAB adsorption curve in Figure 3 is about 1.31 CTAB molecules/nm^2, and this is about 2.2 times higher than the value obtained for the adsorbed amount from a 0.01 mM CTAB solution. The higher amount of CTAB adsorbed corresponds to a more contiguous CTAB structure that is also less patchy in the second layer (admicelles).[9] Addition of 0.5 mM d_{25}-SDS to this CTAB layer results in the expulsion of about 28.5% of the CTAB from the surface and an uptake of about 0.71 d_{25}-SDS molecules/nm^2. In terms of CTAB/SDS number ratio, the final equilibrium value obtained for the mixed surfactant structure on the surface is 1.3 CTAB/SDS. This is lower than the 1.8 CTAB/SDS ratio measured for the uptake of d_{25}-SDS by the adsorbed CTAB hemimicelles. In a separate experiment using nondueterated SDS, a 5 cm^{-1} shift to lower frequency in the CH_2 antisymmetric stretching mode was observed. We recall that the corresponding shift of 4 cm^{-1} was measured for the mixed surfactant structure produced by d_{25}-SDS incorporation into the CTAB hemimicelles. This indicates that a higher packed mixed surfactant structure is produced with the uptake of SDS into the CTAB admicelles. A more highly packed structure produced by the interaction of d_{25}-SDS with CTAB admicelles is consistent with the higher amount of both CTAB and d_{25}-SDS adsorbed on the TiO_2 as well as the more favorable headgroup−headgroup electrostatic interactions as the CTAB/SDS number ratio lowers and approaches a value of 1.

The uptake of d_{25}-SDS in a CTAB structure having a more complete second layer (less gaps than a hemimicelle) occurs by ejecting CTAB molecules from the admicelle to create space for the incoming d_{25}-SDS molecules (see Scheme 3). Given that 28.5% of CTAB is expelled, it is highly unlikely that all the CTAB removed would come solely from the second layer as this would lead to too few CTAB molecules in this second layer to sustain the large uptake of d_{25}-SDS. Also, given a 1.3 CTAB/SDS number ratio, it is more likely that both upper and lower layers of the admicelle structures contain significant levels of CTAB and d_{25}-SDS. As a result, some CTAB in the first layer is removed or transfers to the second layer.

SCHEME 3: Uptake of SDS by CTAB Admicelles

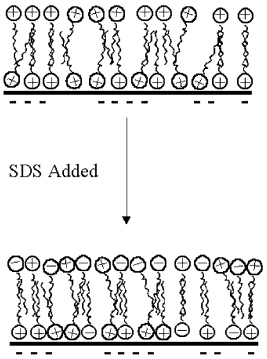

A possible explanation for the uptake of d_{25}-SDS in the first layer of the admicelle is that sections of the admicelle form over regions of the surface that have low or no charged sites. These regions would more easily accommodate mixed surfactant structures. In the case of hemimicelles, the structures are more clustered over charged surface sites, and these regions would be less likely to expel CTAB or accommodate d_{25}-SDS in the first layer.

Interaction of d_{25}-SDS Solution with CTAB Micelles Adsorbed on TiO_2. The CTAB solution concentration used in generating the curve shown in Figure 4 was 1 mM, and this concentration is above the critical micelle concentration (cmc 9.0×10^{-4} M).[17,18] This CTAB solution concentration in contact with the TiO_2 surface leads to an adsorption of about 2.53 CTAB molecules/nm^2. At solution concentrations above the cmc, the high adsorbed amount has been attributed to micelles on the surface.[10] When a 5 mM d_{25}-SDS solution is introduced to this CTAB layer, 63% of the amount of CTAB on the surface was removed, and this was accompanied by the uptake of 0.8 d_{25}-SDS molecules/nm^2. A white precipitate formed in the effluent due to CTAB−SDS salts confirming the expulsion of CTAB from the surface. Because there is a significant percentage of CTAB displaced from the surface, the remaining amount of CTAB and total d_{25}-SDS on the surface is only slightly higher than shown in Figure 3. As a result, the number ratio of CTAB/SDS is only slightly lower at 1.2 CTAB/SDS as compared to the 1.3 CTAB/SDS obtained for adsorption of d_{25}-SDS with CTAB admicelles. When nondeuterated SDS was added, the CH_2 asymmetric band is now shifted lower by 6 cm^{-1}, and this larger shift indicates that mixed surfactant structures are more tightly packed than the mixed surfactant structures produced using lower CTAB and d_{25}-SDS solution concentrations. The picture that emerges is that a mixed micelle structure is formed on the surface (see Scheme 4). This is not surprising as the critical aggregation concentration for mixed CTAB and SDS micelles are two orders in magnitude lower than the cmc for the pure surfactant systems.[10] Since a small percentage of the molecules in a CTAB micelle directly interact with charged sites on the surface, it is anticipated that a high level of expulsion of

SCHEME 4: Uptake of SDS by CTAB Micelles

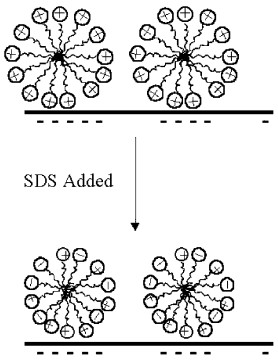

CTAB would occur to accommodate large incorporation of d_{25}-SDS in the mixed micelle structure. It is only in the region near the charged sites on the surface that we anticipate enrichment in CTAB, and this conclusion is supported by spectral data obtained in the headgroup region.

So far, the identification of the mixed surfactant structures was based solely upon changes in the amount of CTAB and d_{25}-SDS adsorbed on TiO_2 and the degree of packing determined from the shift in the CH_2 stretching modes. We now turn our attention to the analysis of the headgroup regions of both d_{25}-SDS and CTAB that should, at least, support the conclusions drawn from the changes in the adsorbed amount. In the next section, we describe the changes occurring in the d_{25}-SDS headgroup region, and this will then be followed by a similar analysis of the CTAB headgroup region.

Headgroup Region of d_{25}-SDS. Figure 5 shows the changes occurring in the headgroup band region of d_{25}-SDS during the uptake of d_{25}-SDS for the 0.01 mM CTAB experiment (i.e., during uptake by the hemimicelle CTAB layer as depicted in Figure 2). Three bands are observed in the headgroup region, two are assigned as S−O antisymmetric stretching bands (ν_{as} S−O) at 1248 and 1221 cm^{-1}, and the third band is the S−O symmetric stretching band (ν_s S−O) at 1038 cm^{-1}. All three bands increase in intensity with incubation time, and this is primarily due to an increase in amount of d_{25}-SDS on the surface (see Figure 2). However, on closer inspection, the spectra clearly show that the ν_{as} S−O band at 1248 cm^{-1} increases at a different rate relative to the lower antisymmetric mode at 1221 cm^{-1}.

Interpretation of the spectral changes of the d_{25}-SDS headgroup in terms of surfactant structures requires an understanding

SCHEME 5: Transition Dipole Moment Vectors for S−O Stretching Modes of SDS

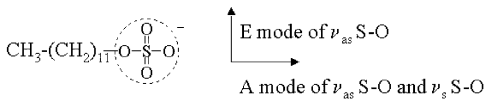

of how these bands respond to changes in their local environment. As with our previous work with CTAB, we rely on the detailed solution studies of mixed CTAB/SDS micelles reported by others.[11,12] In their work, Scheuing and Weers[10] found that the ν_s S−O mode shifted to lower frequency with the loss of interaction of the SDS headgroup with counterions present in the diffuse double layer. The transition dipole moment of the ν_s S−O is located in the direction normal to the micelle surface (see Scheme 5); thus, changes in the counterion density located in the diffuse double layer affect the ν_s S−O band to the greatest extent. Using similar arguments, a direct interaction of the d_{25}-SDS headgroup with charged surface sites or head-to-head adsorption with CTAB should affect the frequency of this band. In the spectra shown in Figure 5, the frequency position of the ν_s S−O band remains constant at 1038 cm^{-1} during the uptake of d_{25}-SDS. This shows that the adsorption of d_{25}-SDS does not occur through vertical head-to-head interaction with the CTAB molecules. On the other hand, a constant ν_s S−O frequency suggests that the uptake of the d_{25}-SDS in the CTAB hemimicelle occurs primarily through lateral surfactant−surfactant interactions as these interactions would occur in a direction that is orthogonal to the transition moment vector of the ν_s S−O band.

In their solution studies, Scheuing and Weers noted that the changes in intensity and frequency position occurring in the ν_{as} S−O bands were more difficult to interpret because this region had two overlapping bands. Nevertheless, in their solution studies with mixed SDS/CTAB micelles, they attributed the splitting and shifting in the ν_{as} S−O bands to a lowering of the symmetry of the SO_4 headgroup resulting from changes in the lateral electrostatic interactions between the SDS and CTAB molecules. In Figure 5, the most significant spectral changes occur in the relative intensity of the two ν_{as} S−O modes. During the initial stage, the 1248 cm^{-1} peak is higher in intensity than the 1221 cm^{-1} peak, whereas at the latter stage the 1221 cm^{-1} peak is more intense than the 1248 cm^{-1} peak. Accordingly, these changes indicate a strong lateral interaction between d_{25}-SDS and CTAB molecules.

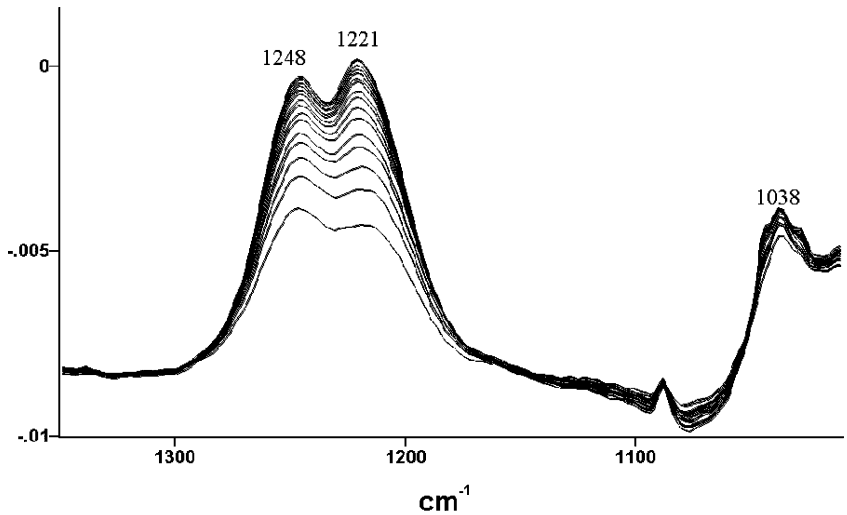

Figure 5. Change in the intensity of the S−O headgroup bands as a function of reaction time during the uptake of d_{25}-SDS into the preadsorbed CTAB layer as described in Figure 2.

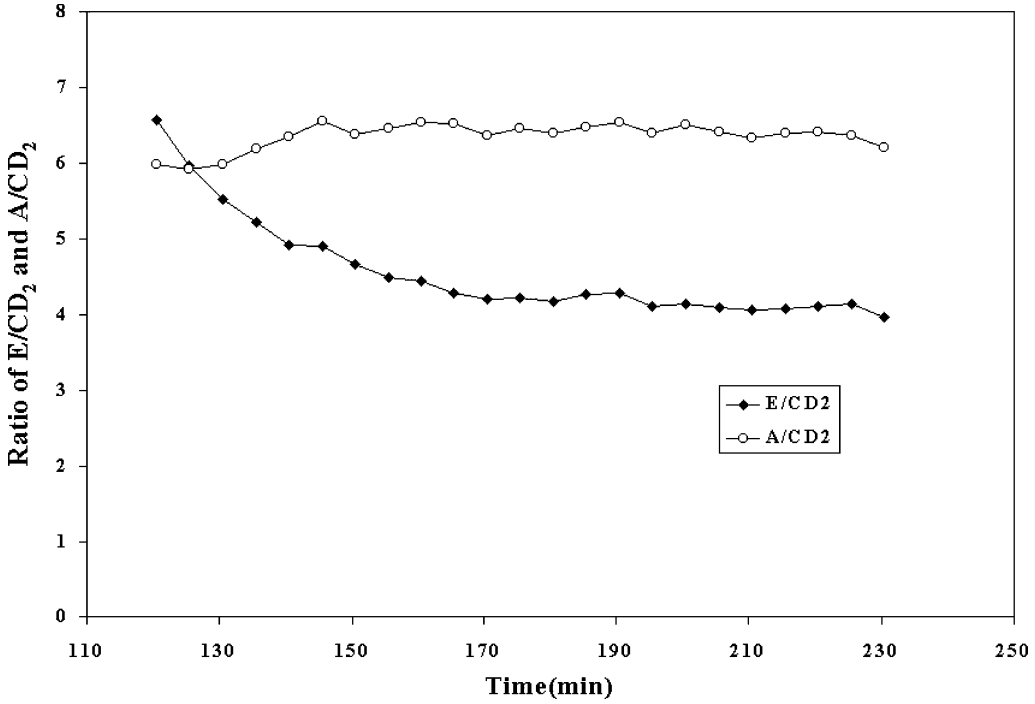

Figure 6. Normalized values of the A (○) and E (◆) ν_{as} S−O modes for the spectra shown in Figure 5.

The structural interpretation of the changes in the two ν_{as} S−O modes put forward by Schuring and Weers was based on the assumption that the transition moment vector for two ν_{as} S−O modes lies parallel to the micelle direction and thus would be sensitive to lateral interactions and changes in the number of adjacent CTAB molecules. However, on closer inspection, the transition moment vectors of the two ν_{as} S−O modes are not in the same direction but rather are normal to each other, which lead us to offer an alterative explanation for interpretation of the spectral changes shown in Figure 5.

Starting with a free sulfate ion belonging to the T_d point group, the ν_{as} S−O mode is a triply degenerate T vibration, and the ν_s S−O band is a nondegenerate A vibration.[19] In SDS, the symmetry of the sulfate headgroup is lowered to the C_{3v} point group, which splits the triply degenerate ν_{as} S−O stretching mode into two bands; one band is a doubly degenerate E vibration and a second nondegenerate A vibration. From spectroscopic considerations, the directions of the dipole moment for the A and E vibrational mode are orthogonal to each other as shown in Scheme 5. Both the ν_{as} S−O band at 1221 cm^{-1} and the ν_s S−O band at 1038 cm^{-1} are A vibrations and are sensitive to changes (either couterions or surface charges) in the direction normal to the micelle surface. Thus, it is anticipated that these two bands will be more sensitive by intimate contact with a charge surface site much like that found for the δ_s $^+N-CH_3$ band for CTAB adsorbed on TiO_2.

Supporting evidence for assignment of the three SDS headgroup bands was provided by a separate experiment in which d_{25}-SDS was introduced to a positively charged TiO_2 surface at pH = 3.5. In this case, the E vibration of the ν_{as} S−O (E ν_{as} S−O) appeared at the same frequency of 1248 cm^{-1} as shown in Figure 5, whereas the two A vibrations (A ν_{as} S−O at 1221 cm^{-1} and A ν_s S−O at 1038 cm^{-1} in Figure 5) shifted to 1205 and 1034 cm^{-1}, respectively. Since the transition dipole moment for both A vibrations is normal to the micelle surface, we would anticipate a shift in frequency for both these bands with adsorption of the d_{25}-SDS headgroups on positively charged surface sites. In contrast, the transition dipole moment for the E ν_{as} S−O vibrational band is in the lateral direction (see Scheme 5) and thus would not be affected by adsorption onto charged sites on the surface.

Returning to Figure 5, it was observed that the two ν_{as} S−O modes show different changes in intensity with time as more d_{25}-SDS is incorporated into the CTAB layer. An initial examination of the spectra in Figure 5 show that the A ν_{as} S−O at 1221 cm^{-1} increases at a faster rate than the E ν_{as} S−O at 1248 cm^{-1}. This would counter the the expected trend as it was anticipated that the intensity of the E ν_{as} S−O would be sensitive and the A ν_{as} S−O insensitive to lateral CTAB−SDS interactions. However, the trend is difficult to discern from Figure 5 because both ν_{as} S−O bands are also increasing due to an increase in the amount of d_{25}-SDS adsorbed on the TiO_2. A more relevant measure from a structure standpoint is the change in intensity of the A and E ν_{as} S−O vibrations normalized to the intensity of the CD_2 band at 2090 cm^{-1}. This normalized value would account for the fluctuation in number of d_{25}-SDS molecules on the surface and thus provide a measure of the average change in the intensity of each headgroup band per d_{25}-SDS molecule.

Figure 6 is a plot of the normalized intensity with time for both ν_{as} S−O modes. This plot shows that the normalized A ν_{as} S−O vibration remains constant, whereas in fact, it is the normalized E ν_{as} S−O vibration that decreases as more d_{25}-SDS is incorporated into the CTAB structure. The ν_s S−O mode at 1038 cm^{-1} (not shown) also has a constant intensity per d_{25}-SDS molecule and shows no shift in frequency with the uptake of d_{25}-SDS. Given the vector orientation of the transition dipole moment for the two ν_{as} S−O bands, the data in Figure 6 show that the incorporation of d_{25}-SDS into the hemimicelle CTAB structure is through lateral surfactant−surfactant interactions.

It is interesting to note that the normalized E ν_{as} S−O band decreases with d_{25}-SDS uptake. One would expect an increase in the normalized E ν_{as} S−O band with a decrease in the average distance between the two oppositely charged headgroups. We recall that there is a shift to lower frequency in the CH_2 stretching modes with increasing uptake of d_{25}-SDS that, in turn,

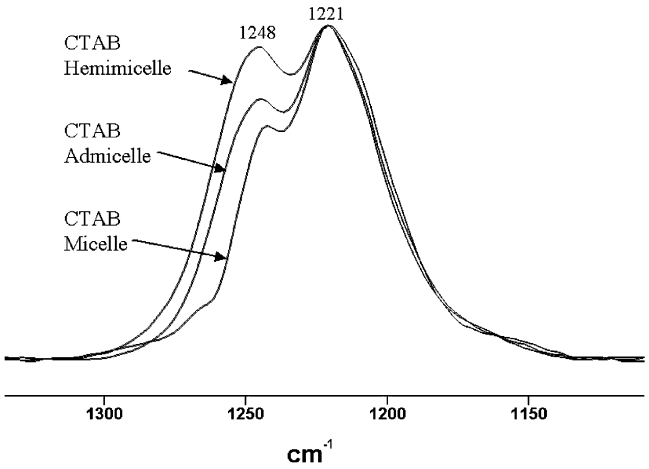

Figure 7. Relative intensity of the ν_{as} S−O modes obtained at equilibrium for addition of d_{25}-SDS to the indicated CTAB structures. The spectra are scaled to the intensity of the band at 1221 cm^{-1}.

translates to an average decrease in the distance between CTAB and d_{25}-SDS headgroups. From this factor alone, an increase and not a decrease in the normalized E ν_{as} S−O band would be expected.

A decrease in the intensity of the normalized E ν_{as} S−O band is also expected for a decrease in the average countercharge density surrounding the d_{25}-SDS headgroup. This is indeed the situation with the uptake of d_{25}-SDS by the CTAB hemimicelle. As more d_{25}-SDS is added into the gaps of the patchy CTAB bilayer, the average number of CTAB molecules surrounding each d_{25}-SDS molecule decreases. Given the trend shown in Figure 6, it would appear that the decrease in the average countercharge density surrounding the d_{25}-SDS headgroup dominants over the average decrease in CTAB/SDS distance in determining the intensity of the normalized E ν_{as} S−O band.

It is anticipated that the previous analysis of the changes in the d_{25}-SDS headgroup bands will provide information on the mixed surfactant structures formed when d_{25}-SDS is added to admicelle and micelle CTAB structures. When d_{25}-SDS is added to all three CTAB structures, it is found that the time-dependent value for the intensity of the normalized E ν_{as} S−O band decreases, and the intensity of the normalized A ν_{as} S−O mode remains constant. This shows that the incorporation of d_{25}-SDS into all three structures on the surface is primarily through lateral surfactant interactions.

There is, however, a difference in absolute intensity of the E ν_{as} S−O mode relative to the A ν_{as} S−O band for the three SDS/CTAB equilibrium structures. This is shown in Figure 7. For comparative purposes, the spectra in Figure 7 are scaled to a constant intensity of the A ν_{as} S−O band at 1221 cm^{-1}. In actuality, the spectra have different absolute intensities because there are different amounts of adsorbed d_{25}-SDS. In Figure 7, the value calculated for the intensity ratio of the normalized E ν_{as} S−O/CD_2 bands was 4, 2.75, and 1.28 for uptake of d_{25}-SDS by the hemimicelle, admicelle, and micelle CTAB structures, respectively. We recall that the intensity of the E ν_{as} S−O vibration depends on two factors: the average number of surrounding CTAB molecules and the CTAB/SDS headgroup−headgroup distance. From the frequency shift of the CH_2 symmetric mode, the packing density for adsorption of d_{25}-SDS by CTAB micelles is higher than CTAB admicelles or hemimicelles. Thus, the proximity of d_{25}-SDS and CTAB headgroups would be the closest in the mixed micelle structure, and from this standpoint alone, this would lead to the highest value for

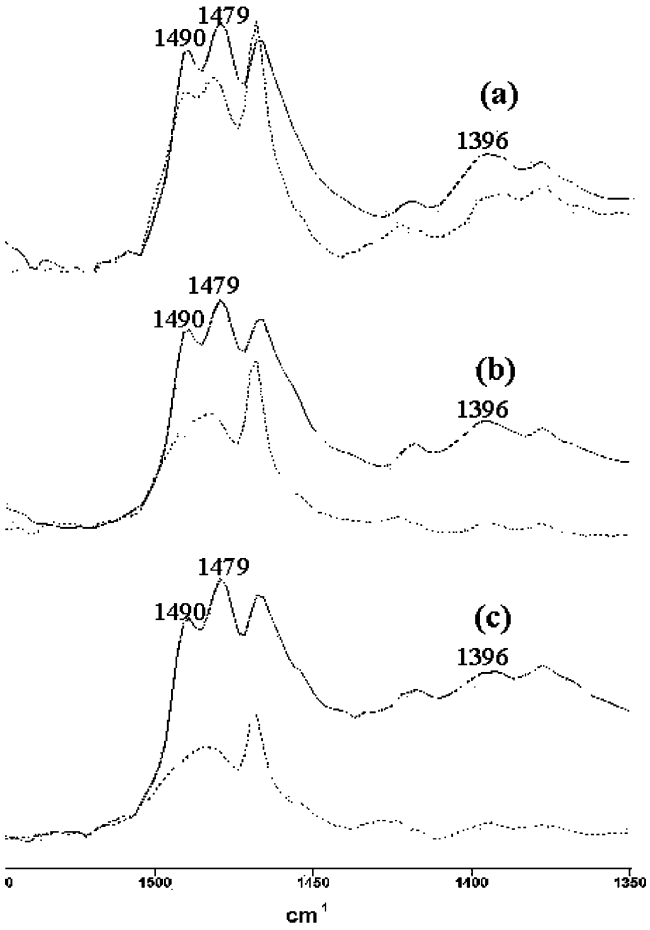

Figure 8. IR bands of CTAB headgroup before (solid curve) and after d_{25}-SDS addition (dashed curve) for adsorbed CTAB using CTAB solution concentrations of (a) 0.01 mM, (b) 0.1 mM, and (c) 1mM.

the intensity of the normalized E ν_{as} S−O band. However, the lowest value is obtained for the normalized E ν_{as} S−O vibration with addition of d_{25}-SDS to preadsorbed CTAB micelles. Thus, as found for the uptake of d_{25}-SDS by the CTAB hemimicelle, the dominant factor contributing to the overall intensity of the E ν_{as} S−O band is the relative number of CTAB molecules surrounding the d_{25}-SDS molecule. The number ratio of CTAB/SDS decreases from 1.8, to 1.3, to 1.2 for addition of d_{25}-SDS to CTAB hemimicelles, admicelles, and micelles, respectively, and this is consistent with the trend in the normalized E ν_{as} S−O values. In effect, the addition of d_{25}-SDS to the CTAB micelles has a lower average number of CTAB surrounding the d_{25}-SDS molecule leading to the lowest value for the normalized E ν_{as} S−O intensity.

CTAB Headgroup. It is also anticipated that formation of the mixed SDS/CTAB structures would also lead to a perturbation of the CTAB headgroup bands. Figure 8 shows the headgroup CTAB spectral region just before addition of d_{25}-SDS and recorded at the equilibrium point after d_{25}-SDS addition for all three CTAB concentrations. The key headgroup bands are assigned as δ_{as} $^{+}N-CH_3$ at 1490 and 1479 cm^{-1} and the δ_s $^{+}N-CH_3$ at 1396 cm^{-1}.[6] All other bands are various CH_2 and CD_2 modes.

For all three cases, the δ_{as} $^{+}N-CH_3$ bands at 1479 and 1490 cm^{-1} change in position and shape with the uptake of d_{25}-SDS. The change in these bands is most pronounced with the uptake of d_{25}-SDS by the CTAB micelles and admicelles that results in the appearance of a broad ill-defined feature at 1482 cm^{-1}. The transition dipole moment for the δ_{as} $^{+}N-CH_3$ modes lie

in the same direction[9,11] as the *E* ν_{as} S−O vibration of the d_{25}-SDS headgroup and thus is affected by lateral surfactant−surfactant interactions. The change in the δ_{as} $^{+}N-CH_3$ is less with d_{25}-SDS addition to adsorbed CTAB hemimicelles than either adsorbed CTAB admicelles or micelles, and this is consistent with the trend in the *E* ν_{as} S−O band.

Of particular note are the changes that occur in the 1396/2850 ratio. The transition dipole moment for the 1396 cm^{-1} band (δ_s $^{+}N-CH_3$) is in the same direction as the *A* vibrations of the ν_{as} S−O and ν_s S−O bands. Changes to the 1396/2850 ratio have been shown to be sensitive to the number of CTAB directly interacting with the surface.[9] Addition of d_{25}-SDS to adsorbed CTAB micelles leads to an increase in the 1396/2850 ratio, and this means that a higher proportion of the remaining CTAB are bound to oppositely charged surface sites. This is not surprising as 63% of the CTAB are ejected from the surface with addition of the d_{25}-SDS, and it would be more easy to eject those CTAB molecules in the sections of the micelle that are not in intimate contact with charged surface sites. We recall that the picture obtained from the shift in the CH_2 symmetric mode along with the spectral data form the d_{25}-SDS headgroup suggests a tightly aggregated mixed micelle adsorbed on the surface. A higher 1396/2850 ratio shows that this mixed micelle is not uniformly distributed but rather is enriched in CTAB near the surface. In effect, the incoming d_{25}-SDS occupies regions of the outer micelle in a higher concentration than the area near the surface containing the CTAB that are bound to the negative surface sites. This gives rise to CTAB enriched micelle (the CTAB/SDS number ratio was 1.2).

In contrast to the addition of d_{25}-SDS to CTAB micelles, the 1396/2850 ratio decreases slightly for both addition of d_{25}-SDS to CTAB hemimicelles and addition of d_{25}-SDS to admicelles. The reduction of this ratio shows that a fewer percentage of the remaining CTAB on the surface are in direct contact with charged surface sites. This implies that some of the adsorbed CTAB in the first layer of both the adsorbed hemimicelle and the adsorbed admicelle rearranges to the upper layer to interact with the d_{25}-SDS.

Conclusions

The subtle changes in the infrared bands due to surfactant headgroups provide a unique insight to the aggregated structures of mixed surfactants on charged metal oxide surfaces. Both CTAB and SDS headgroup contain bands with transition dipole vectors that are orthogonal to each other. It is found that bands whose transition dipole vectors lie parallel to the micelle surface (δ_{as} $^{+}N-CH_3$ CTAB bands at 1479 and 1490 cm^{-1} and ν_{as} S−O band of SDS at 1248 cm^{-1}) change in intensity/position due to lateral−lateral interactions. In contrast, bands whose transition dipole vectors are perpendicular to the surface (δ_s $^{+}N-CH_3$ band at 1396 cm^{-1}, ν_{as} S−O band at 1221 cm^{-1}, and ν_s S−O band at 1038 cm^{-1}) are sensitive to head−head interactions between surfactants and with adsorption onto charged surface sites. Combining the spectroscopic information from the headgroup region with the measurement of the adsorbed amount obtained from bands due to the alkyl tails has resulted in a clearer understanding of the interaction of mixed surfactants on surfaces.

References and Notes

(1) Myers, D. *Surfactant Science And Technology*; VCH: New York, 1992.
(2) Sjoberg, M.; Bergstrom, L.; Larsson, A.; Sjostrom, E. V. A. *Colloids Surf., A* **1999**, *159*, 197.
(3) Kolesnikova, T. P.; Polunina, I. A.; Roldughin, V. I. *Colloid J.* **2002**, *64*(3), 319.
(4) Sidorova, M.; Golub, T.; Musabekov, K. *Adv. Colloid Interface Sci.* **1993**, *43*, 1.
(5) Thorstenson, T. A.; Tebelius, L. K.; Urban, M. W. *J. Appl. Polym. Sci.* **1993**, *50*, 1207.
(6) Ninness, B. J.; Bousfield, D. W.; Tripp, C. P. *Colliods Surf., A* **2002**, *203*, 21.
(7) Vander Linden, C.; Van Leemput, R. *J. Colloid Interface Sci.* **1978**, *67*, 48.
(8) Ninness, B. J.; Bousfield, D. W.; Tripp, C. P. *Appl. Spectrosc.* **2001**, *55*, 655.
(9) Li, H.; Tripp, C. P. *Langmuir* **2002**, *18*, 9441.
(10) Scheuring, D. R.; Weers, J. G. *Langmuir* **1990**, *6*, 665.
(11) Weers, J. G.; Scheuing, D. R. In *Micellar sphere to rod transitions, Fourier transform infrared spectroscopy in colloid and interface science*; Scheuing, D. R., Ed.; American Chemical Society: Washington, DC, 1990.
(12) Yang, P. W.; Mantsch, H. H.; Baudais, F. *Appl. Spectrosc.* **1986**, *40*, 974.
(13) Neivandt, D. J.; Gee, M. L.; Hair, M. L.; Tripp, C. P. *J. Phys. Chem. B* **1998**, *102*, 5107.
(14) Neivandt, D.; Gee, M. L.; Tripp, C. P.; Hair, M. L. *Langmuir* **1997**, *13*, 2519.
(15) Harrick, N. J. *Internal Reflection Spectroscopy*; John Wiley & Sons: New York, 1987.
(16) Velegol, S. B.; Fleming, B. D.; Biggs, S.; Wanless, E. J.; Tilton, R. D. *Langmuir* **2000**, *16*, 2548.
(17) Wang, W.; Li, L.; Xi, S. *J. Colloid Interface Sci.* **1993**, *155*, 369.
(18) Weers, J. G.; Scheuing, D. R. In *Micellar Sphere to Rod Transitions, Fourier Transform Infrared Spectroscopy in Colloid and Interface Science*; Scheuing, D. R., Ed.; American Chemical Society: Washington, DC, 1991.
(19) Nakamoto, K. *Infrared and Raman Spectra of Inorganic and Coordination Compounds*; John Wiley and Sons: New York, 1986.